# Terahertz Emission From Tubular Pb(Zr,Ti)O3 Nanostructures

**ARTICLE** *in* NANO LETTERS · JANUARY 2009

Impact Factor: 13.59 · DOI: 10.1021/nl802277k · Source: PubMed

NANO LETTERS



Letter

# Terahertz Emission from Tubular Pb(Zr,Ti)O Nanostructures

J. F. Scott, H. J. Fan, S. Kawasaki, J. Banys, M. Ivanov, A. Krotkus, J. Macutkevic, R. Blinc, V. V. Laguta, P. Cevc, J. S. Liu, and A. L. Kholkin

*Nano Lett.*, **2008**, 8 (12), 4404-4409 • Publication Date (Web): 01 November 2008



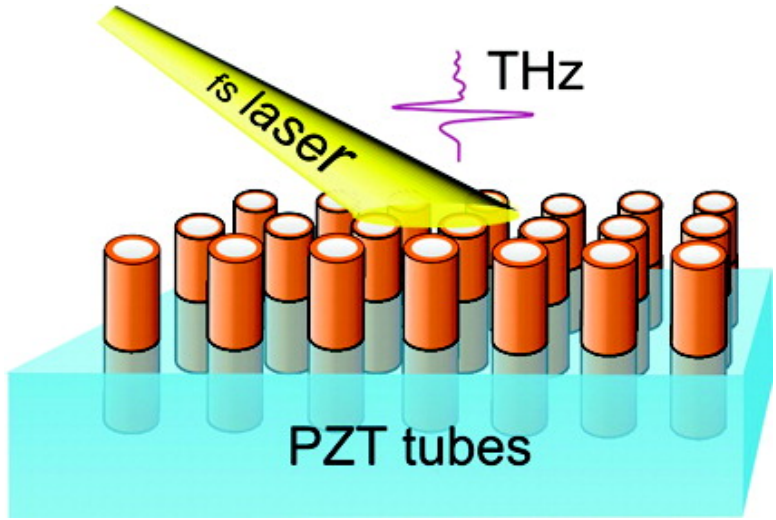


## More About This Article

Additional resources and features associated with this article are available within the HTML version:

- Supporting Information
- Access to high resolution figures
- Links to articles and content related to this article
- Copyright permission to reproduce figures and/or text from this article

View the Full Text HTML

NANO LETTERS

2008
Vol. 8, No. 12
4404-4409

# Terahertz Emission from Tubular $Pb(Zr,Ti)O_3$ Nanostructures

**J. F. Scott,*,† H. J. Fan,†,▽ S. Kawasaki,†,○ J. Banys,‡ M. Ivanov,‡ A. Krotkus,§ J. Macutkevic,§ R. Blinc,|| V. V. Laguta,⊥ P. Cevc,|| J. S. Liu,# and A. L. Kholkin#**

*Department of Earth Sciences, University of Cambridge, CB2 3EQ Cambridge, United Kingdom, Faculty of Physics, Vilnius University, Sauletekio Str. 9, LT-10222 Vilnius, Lithuania, Semiconductor Physics Institute, A. Gostauto str. 11, LT-01108 Vilnius, Lithuania, J. Stefan Institute, Jamova 39, 1000 Ljubljana, Slovenia, Institute of Physics, AS CR, Cukrovarnicka 10, 16253 Prague, Czech Republic, Department of Ceramics and Glass Engineering & CICECO, University of Aveiro, 3810-193 Aveiro, Portugal*

*Received July 28, 2008; Revised Manuscript Received September 20, 2008*

## ABSTRACT

**We report intense terahertz emission from lead zirconate titanate (PZT) tubular nanostructures, which have a wall thickness around 40 nm and protrude on n-type Si substrates. Such emission is totally absent in flat PZT films or bulk; hence the effect is attributed to the nanoscale geometry of the tubes. The terahertz radiation is emitted within 0.2 ps, and the spectrum exhibits a broad peak from 2 to 8 THz. This is a gap in the frequency spectrum of conventional semiconductor terahertz devices, such as ZnTe, and an order of magnitude higher frequency peak than that in the well-studied p-InAs, due to the abnormally large carrier concentration gradient in the nanostructured PZT. The inferred mechanism is optical rectification within a surface accumulation layer, rather than the Dember effect. The terahertz emission is optically pumped, but since the tubes exhibit ferroelectric switching, electrically driven emission may also be possible. EPR reveals $O_2$ molecules adsorbed onto the nanotubes, which may play some role in the emission.**

Terahertz (THz) emission or detection has attracted considerable attention in the past decade because of its promising applications in medical and biological imaging and security controls (see review articles[1,2] and a recent special issue on terahertz emission in ref 3). It roughly corresponds to a frequency range of 0.1−10 THz (3 mm to 30 $\mu$m). Generally, terahertz radiation is generated from a [110] cut ZnTe single crystal through the nonlinear process of optical rectification. This gives a spectrum extending from 0.1 to 2.5 THz. However, nowadays high-energy ultrashort terahertz pulses are strongly desired particularly for the security imaging and nonlinear terahertz spectroscopy applications. Until recently only free-electron laser sources[4] and femtosecond optical pump systems with ferroelectric $LiNbO_3$ emitters[5] have been able to generate terahertz pulses that have at least 1 $\mu$J of energy.

Lead zirconium titanate (PZT) is a most typical ferroelectric material that shows a high potential for piezoelectric device applications due to its high dielectric constant, high Curie temperature, and high breakdown strength. PZT thin films are also widely used as infrared sensors.[6] Our new work suggests that terahertz emitters and detectors based on PZT (via the optical rectification effect) can be produced. Nevertheless so far no data on such emitters or detectors have been published. Two problems exist with the construction of ferroelectrics-based terahertz emitters or detectors: (i) terahertz absorption; and (ii) the velocity mismatch between terahertz and optical signals.[7] There are two possible ways to solve the velocity mismatch problem: pulse front tilting[8] and domain engineering.[9] Nevertheless, the velocity mismatch problem is strongly related to a critical size for ferroelectricity. Mean-field theory predicts the existence of a critical size equal to the ferroelectric correlation length. It can be interpreted as bulk ferroelectricity suppressed by surface depolarization energies and implies that the bulk transition has a minimum critical size. The other approach is based on the surface energy, connected with the truncation of the crystal, and it predicts different estimates for the dielectric properties. These considerations have been used to calculate a critical size, which is about 2.5 nm for small spherical particles or thin films of PZT.[10]

* Corresponding author. E-mail: jsco99@esc.cam.ac.uk.
† University of Cambridge.
‡ Vilnius University.
§ Semiconductor Physics Institute.
|| J. Stefan Institute.
⊥ AS CR.
# University of Aveiro.
▽ Present address: Division of Physics and Applied Physics, SPMS, Nanyang Technological University, 21 Nanyang Link, 637371, Singapore.
○ Present address: Samco Corp., 36 Waraya-cho, Takeda, Fushimi-ku, Kyoto 612-8443, Japan.

10.1021/nl802277k CCC: $40.75 
**Published on Web 11/01/2008**

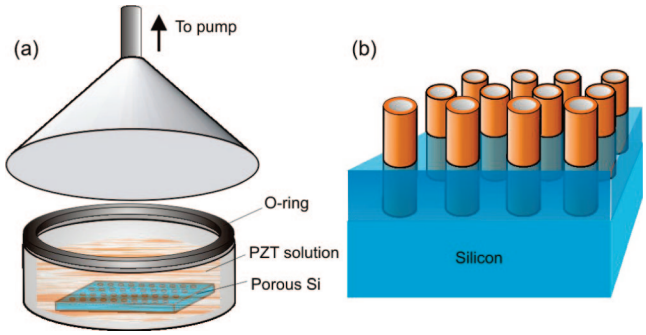


**Figure 1.** Schematics of the (a) fabrication process of PZT tube array in the silicon matrix and (b) the sample structure. A slightly low pressure is created above the MOD-type $Pb(ZrTi)O_3$ solution to assist the infiltration into the pores.

In this Letter we present the first characterization of tubular PZT nanostructures (for convenience, we call nanotubes hereafter) by terahertz reflectivity spectroscopy. Ferroelectricity exists in the PZT nanotubes, as revealed by hysteretic switching, and it is supported by the observation of terahertz radiation generated by the nanotubes at femtosecond laser illumination. It is noted that, compared to extensive terahertz studies on single crystal and superlattice films of electro-optic semiconductors (ZnTe, GaAs-based and GaN-based), as well as ferroelectric relaxors,[11−13] there are relatively few works on nanostructures of these materials. Parkinson et al.[14] investigated the time-resolved conductivity of isolated GaAs nanowires by optical-pump terahertz-probe time-domain spectroscopy. Using a similar terahertz spectroscopy technique, Baxter and Schmuttenmaer[15] measured the terahertz absorption coefficient, index of refraction, and conductivity of ZnO nanowires.

**Fabrication of PZT Tubes.** The PZT tubes were fabricated by solution infiltration of porous Si templates with 4 wt% metalorganic-decomposition type $Pb(Zr_{0.4}Ti_{0.6})O_3$ precursor. The Si used for fabrication of porous template was doped with phosphorus giving a resistivity of 10 Ω·cm. The pores are ordered in hexagonal array, with a 1 $\mu$m diameter, 2 $\mu$m interpore separation, and 20 $\mu$m depth. The porous Si templates were immersed into the solution for 3 min. A slightly low pressure is created above the solution (see Figure 1), analogous to the previously published method.[16] Deposition was also made without vacuum, in which case the substrates are immersed in the solution for about 30 min. After deposition, the samples were dried at 80 °C for about 10 min and then heated at 300 °C for another 10 min. This procedure was repeated twice. Finally, the samples were annealed in a resistive furnace at 650 °C for 20 min (samples were inserted into the preheated tube) during which the PZT crystallizes and the tube wall has a polycrystalline perovskite structure.[16,17] The composition used was close to the morphotropic phase boundary $x = 0.48$.

In order to partially expose the PZT tube arrays from the Si matrix, the sample was mechanically polished (to remove surface PZT layer), sonicated (to remove particles aggregated at the pore openings), and dipped in a 30 wt % KOH solution at room temperature for 1 h (to etch the Si matrix). The tubes

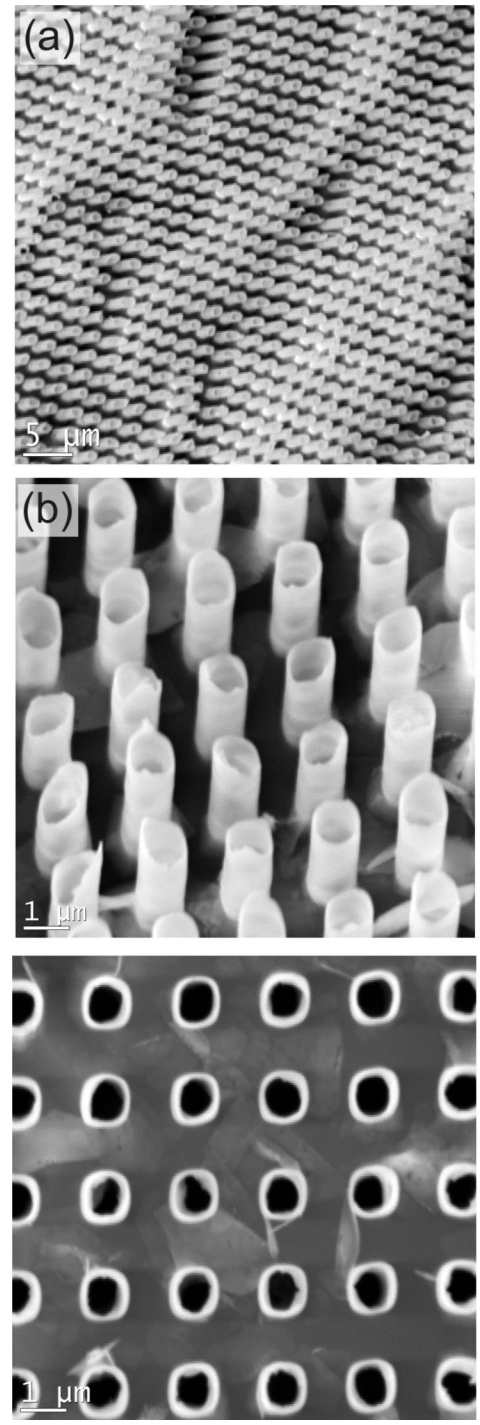


**Figure 2.** Scanning electron microscopy images of the PZT nanotube array protruding from the Si substrate. Note that the tube openings are unsmooth due to breaking by sonication. (a, b) Tilted view at different magnifications. (c) Top view of (b).

obtained have a wall thickness of 45 ± 5 nm. The exposed part of the tubes is about 3 $\mu$m high, while the remaining parts of the tubes are embedded within the Si. Figure 2 shows the representative scanning electron microscopy images of the PZT tube array. The tubes (see Figure 2) had a circular cross section with 1 $\mu$m in total diameter and was tilted by 20° with respect to the plane of the substrate.

**Terahertz Emission.** Figure 3 shows schematically the experimental setup for terahertz emission with laser excitation

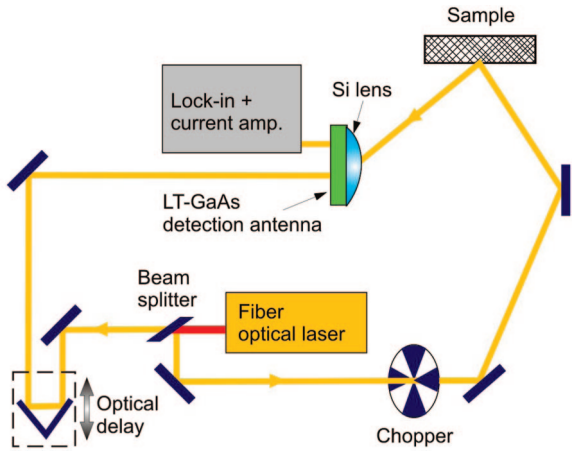


**Figure 3.** Experimental setup for the THz emission experiment with laser excitation from the surface.

from the surface: A fiber-optic laser delivers pulses of 70 fs duration at a wavelength of 800 nm with 90 MHz repetition rate. The pump beam was incident at 45° to the sample surface. The average pump laser power was ~40 mW. THz radiation was focused by means of a Si lens and collected by a photoconductive detector. The detector was fabricated from the layer of GaAs grown by molecular beam epitaxy at low (~250 °C) substrate temperature.

Figure 4 shows the time-domain waveforms measured on a PZT nanotube sample (sample 7a) and its corresponding fast-Fourier transform spectra. The traces labeled 5a are for an identical porous Si substrate but with no PZT and exhibit only noise. The terahertz radiation is emitted within 0.2 ps, and the spectrum exhibits a broad peak from 2 to 8 THz, with maximal amplitude at 3 THz. Similar to other nonlinear materials (e.g., $LiNbO_3$ and ZnTe)[5,18] the main terahertz generation mechanism in PZT nanotubes is optical rectification.

Generally, the width of the main terahertz pulse is similar to the width of pumped femtosecond pulses, because the emitted terahertz electric field $E(t)$ is proportional to excited photocurrent: $E(t) \sim \partial J(t)/\partial t$. However, due to some dynamics processes (scattering, etc.) and dispersion, the emission pulse is usually longer than the pumping impulse. Nevertheless these processes can be negligible, and the duration of terahertz impulses can be similar to the pumping impulse duration and also easily can be measured by a standard terahertz measurement technique.[19]

Terahertz emission in electro-optic crystals has been studied in the past in a variety of semiconductors. Following the 1992 report by Zhang and Auston[20] there were several models proposed, basically involving optical rectification[21] or the optical Dember effect.[22] In some cases the effect is due to optical rectification and in particular the response of the gradient in carriers produced within the surface accumulation layer in p-InAs is moot—possibly due to carrier gradients and optical rectification and possibly due to[23] the Dember effect. However, for wide-bandgap materials such as PZT ($E_g = 3.6$ eV), the photo-Dember effect should be negligible, because the absorption depth is relatively deep. In the present study the terahertz spectrum is similar to that known in p-InAs [100] crystals but shifted to a frequency range about 1 order of magnitude higher, which could be useful for agile frequency devices. This increase in frequency arises from the abnormally large carrier concentration gradient in PZT, which decreases from $3 \times 10^{20}$ cm$^{-3}$ at the surface to $5 \times 10^{18}$ cm$^{-3}$ in the interior of the film, only 20 nm deep.[24] This is due to oxygen vacancy concentration and is orders of magnitude greater than that in any conventional III−V or II−VI semiconductor. In addition, the carrier mobility $\mu$ in PZT is much lower, of order $10^{-6}$ cm$^2$/V•s, which further increases the carrier concentration gradient near the surface when subjected to femtosecond laser pulses, in comparison with InAs.[25]

A useful but oversimplified expression for peak terahertz emission frequency is

$$f(\text{peak}) = B\mu^{-1} \nabla n \tag{1}$$

and for intensity

$$I = C \nabla n d_{jj} \tag{2}$$

where $d_{jj}$ is the diagonal piezoelectric tensor component for direction $j$ normal to the surface, and $B$ and $C$ are constants.

In terms of basic physics, the terahertz radiation intensity from semiconductors has always been thought to be proportional to the piezoelectric coefficient,[20] as seen from eq 2. In hindsight, therefore, strong emission from PZT nanotubes with 40 nm thick walls is not surprising, because PZT is one of the best known piezoelectrics ($d_{33}$ ~50 pm/V). Fabricating a material with extremely large $d_{33}$ coefficient and an abnormally large carrier concentration gradient$\nabla n$ near the surface into a 40 nm thick nanotube thus optimizes the parameters requisite for terahertz emission.

In semiconductor terahertz devices, it is also important that the carrier mobility be high (e.g., $\mu_h \approx 4400$ cm$^2$/V•s and $\mu_e \approx 850$ cm$^2$/V•s for semi-insulating GaAs[26]). The mobility of electrons and holes in bulk PZT are typically small, with $\mu_h = 2.93 \times 10^{-6}$ cm$^2$/V•s (hole[27]); however, some authors report very high surface mobilities,[28−30] and this could help explain why the phenomena reported here are observed in only nanogeometry devices (for which the surface/volume ratio is extremely high).

**Terahertz Reflectivity.** Since the Si substrates were n-type doped (with a doping density of $5 \times 10^{15}$ cm$^{-3}$), they were opaque in terahertz range and thus unsuitable for a terahertz transmission experiment. We performed reflectivity measurements with a terahertz spectrometer based on an optically pumped terahertz laser (Edinburg Instruments[31]) and with a highly sensitive pyroelectric terahertz detector.

Terahertz reflectivity was measured both from an empty porous Si surface and from the Si surface with protruding PZT nanotubes at different frequencies in the range of 0.5−6.5 THz and temperatures of 4−300 K and using three kinds of excitation wavelengths. Figure 5 shows that for both samples the terahertz reflectivity increases on cooling. This increase is mainly due to the increase of the Si conductivity. A similar increase attributed to carrier mobility was reported for p-InAs by Mendis et al.[32]

**Electric Switching of PZT Tubes.** The present terahertz studies were carried out with optically driven signals from

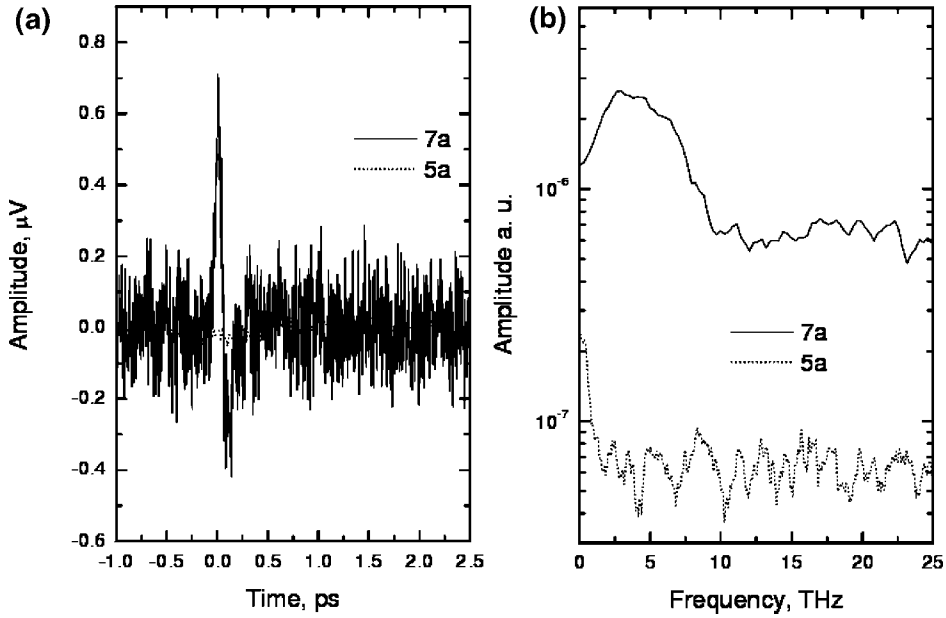


**Figure 4.** (a) Wave form and (b) spectra of a terahertz pulse generated from PZT nanotubes (sample 7a). The dashed line denotes trace from a sample without PZT nanotubes.

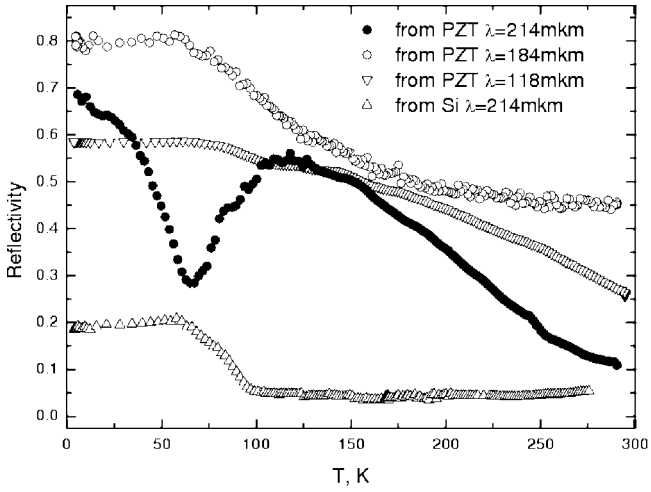


**Figure 5.** Temperature-dependence of terahertz reflectivity from a Si surface with PZT nanotubes and from an empty porous Si substrate.

an femtosecond laser. However, practical devices would be better made if the terahertz could be electrically driven with an applied voltage. We can in fact alter the near-surface electrical parameters very rapidly by switching the ferroelectric nanotubes using piezoresponse force microscopy (PFM). The result is shown in Figure 6. Although switching of PZT nanotubes has been reported before,[17,33,34] Figure 6a is the first to map out the response for each location on top of the nanotube and for different positions on the inside wall (in the figure the outside nanotube wall is electroded to ground, and the applied voltage is through an AFM/PFM tip; the polarization is proportional to the effective $d_{ij}$ piezoelectric coefficient and is minimum in the area shown as black in the figure). The hysteresis loop measured on the tube wall (Figure 6b) is the clear proof of ferroelectric switching and strong electrostatic effect due to measurement geometry. The terahertz generation reported in the present paper is entirely laser-driven, same as most terahertz emission devices, but the demonstration of electric switching in the same nanotubes suggests that it should be possible to fabricate voltage-triggered terahertz emission as well.

**Electron Paramagnetic Resonance of PZT Nanotubes.** Because of the interesting terahertz properties of our PZT nanotubes and their dependence upon surfaces and surface-to-volume ratios, it seemed worthwhile to investigate the local structure of these nanotubes by electron paramagnetic resonance (EPR).

Two different samples were studied. The first one consists of PZT nanotubes together with the Si substrate (see Figure 2). The second one was the same sample but the PZT nanotubes were brushed off by polishing so that no PZT tubes protrude the Si substrate. The corresponding X-band EPR spectra are shown in Figure 7. As can be seen, there is only a weak EPR spectrum in the pure substrate and a rather strong one in the sample with nanotubes. The nanotube spectrum is asymmetric (Figure 7) and extends from about 4000 to 12500 G with a maximum around 12000 G. The spectrum is unobservable at higher temperatures due to strong increase of the microwave absorption by the Si substrate.

As a control experiment, pure $SiO_2$ tubes without PZT, which was obtained by thermal oxidation of a porous Si substrate at 1200 °C plus KOH etching, was also studied. No EPR signal was observed.

Such an unusual EPR spectrum can be attributed to free or quasi-free $O_2$ molecules absorbed into the nanotubes. A similar spectrum is often observed even from ambient air in the cavity of the spectrometer. At low air pressure (1−10 mmHg) the resonance lines are narrow and up to 120 lines can be easily resolved at the magnetic field region 1400−11000 G.[35] Such a large number of transitions is caused by quantization of the rotational magnetic moment of the $O_2$ molecule. With increase of the pressure, the

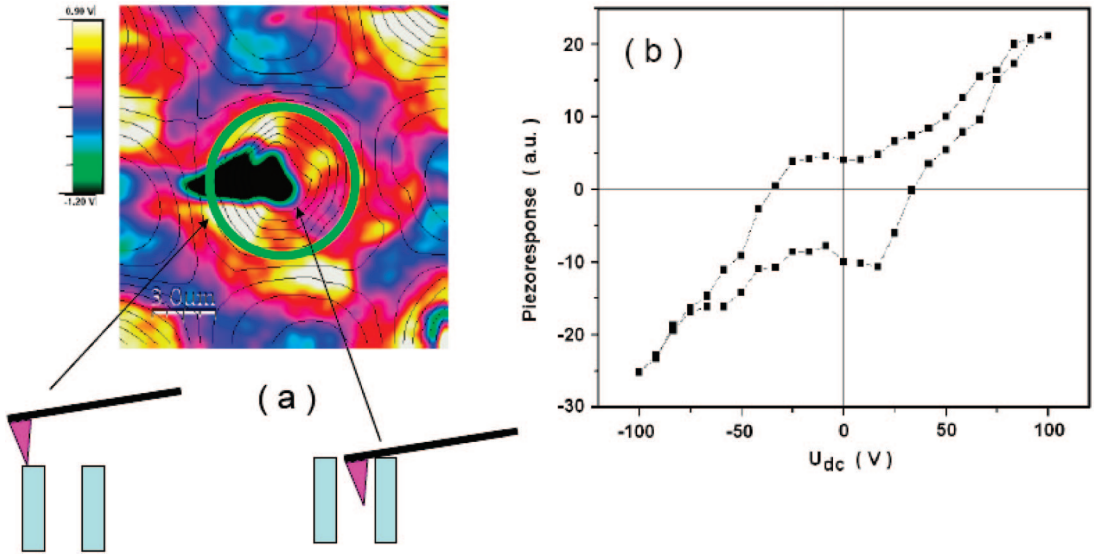


**Figure 6.** (a) Piezoresponse maps of PZT tube arrays with superimposed (black contours) topography. The schematics show the cantilever positions and illustrates inability to image piezoresponse in the black area. Different colors correspond to different strength of the piezoresponse signal. (b) Representative ferroelectric hysteresis loop taken on the tube wall.

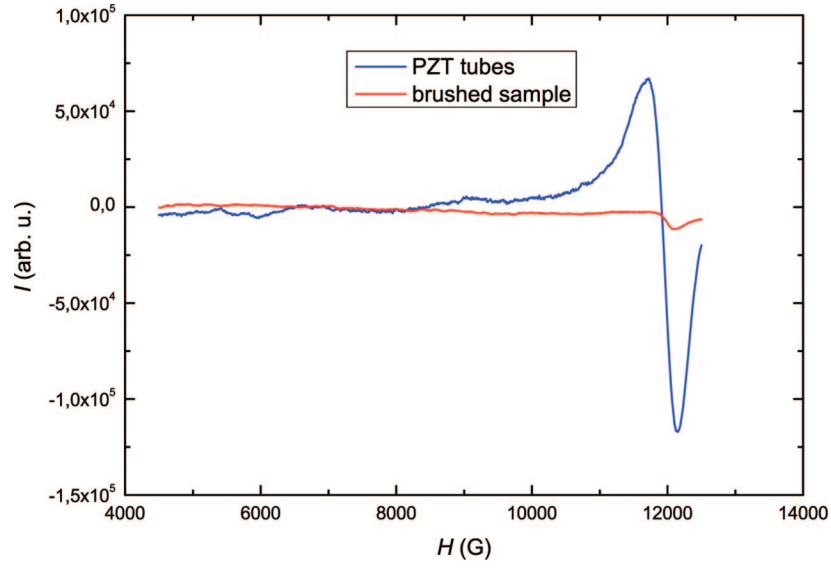


**Figure 7.** EPR spectra from a $Si/SiO_2$ substrate with PZT nanotubes (blue line) and from only a substrate (red line) measured at 12 K. The spectrum is attributed to $O_2$ molecules absorbed into nanotubes.

resonance lines become very broad due to the magnetic interaction between molecules and finally all resonances merge into one broad spectrum. Because our measurements were performed with a cavity inserted into He cryostat, where air is displaced by pure He, the observed spectrum is indeed produced by the nanotube arrays and not by oxygen from air.

We have acquired additional data that are helpful in identifying the $O_2$ signal. It is important that the $O_2$ signal has an additional EPR line around 4000 G. Subsequently we found a stronger line at high field. It is unambiguously molecular oxygen trapped inside a microcavity. Our spectra match closely that identified from the oxygen center in microcavities of amorphous aluminum borate,[36] in which case the signals have quite different values than for free $O_2$. Therefore we interpret the center as oxygen molecules trapped inside the PZT nanotubes and not adsorbed onto the outer surfaces.

It should be noted that OH molecular radicals[37] can also contribute into the spectrum shown in Figure 7. However, value of this contribution can hardly be determined from the measured spectrum.

As it was mentioned above, PZT films (and with high probability nanotubes too) are characterized by a large carrier concentration at the surface.[24] One can expect that the carriers are trapped by oxygen vacancies and thus form F and $F^+$ centers. Therefore, some of the weak powder-like resonance lines at magnetic field 4000−6000 G could be created by the paramagnetic $F^+$ center, where the trapped electron is predominantly localized at $Ti^{3+}$ ion as it takes place, for example, in $BaTiO_3$ (ref 38) or $PbTiO_3$.[39] Further detailed EPR investigation with use of $Al_2O_3$ substrates is necessary

for convincing separation of the $F^+$ center (and maybe other intrinsic defects created at tube surface) resonances because in the present study Si substrate limited the temperature range of the EPR measurements within 4.2−20 K due to large microwave absorption of Si at higher temperatures.

**Conclusions.** We have provided THz emission spectra from an array of PZT nanotubes. This shows the potential for filling the spectral gap from 2−10 THz generally not satisfied by conventional semiconductor devices. THz emission has been reported previously for another ferroelectric oxide ($BiFeO_3$), but only for flat films,[43,44] whereas our PZT THz signals disappear for flat films (note that the THz spectrum of PZT and PLZT is well known from earlier work by some of us[45]). Although the present work involves short-pulse laser initiation, the fact that the same ferroelectric nanotubes switch ferroelectrically, and therby change their near-surface electrical characteristics dramatically (shown elsewhere to occur in as little as 250 ps at high fields) suggests that voltage-driven devices might also be possible.

The inference that the PZT surfaces are critical to the terahertz performance has led us to examine their surface physics, including adsorbed molecules and ions. Careful study of the PZT nanotube surfaces via EPR reveals adsorbed $O_2$ molecules, but it is not clear what role if any they play in the terahertz emission characteristics.

The new results are exciting because previously such high frequencies were generated primarily with quantum wells;[40] PZT nanotubes are much cheaper and easier to process, certainly compared with expensive $Hg_{1-x}Cd_xTe$ films on CdZnTe substrates,[41,42] which is a commercial advantage of PZT for terahertz generators.

**Acknowledgment.** We thank Dr. A. Langner, Max Planck Institute of Microstructure Physics (Germany), for providing the Si substrates. The work in Cambridge, Vilnius, Aveiro, and Ljubljana was all supported by EU STREP "Multiceral".

## References

(1) Davies, A. G.; Burnett, A. D.; Fan, W. H.; Linfield, W. H.; Cunningham, J. E. *Mater. Today* **2008**, *11*, 18–26.
(2) Federici, J. F.; Schulkin, B.; Huang, F.; Gary, D.; Barat, R.; Oliveira, F.; Zimdars, D. *Semicond. Sci. Technol.* **2005**, *20*, S266−S280.
(3) Special issue on heterostructure terahertz devices: *J. Phys. Condens. Mater.* **2008**, *20*, 380301−384211.
(4) Knippels, G. M. H.; Yan, X.; MacLeod, A. M.; Gillespie, W. A.; Yasumoto, M.; Oepts, D.; van der Meer, A. F. G. *Phys. Rev. Lett.* **1999**, *183*, 1578–1581.
(5) Yeh, K. L.; Hoffmann, M. C.; Hebling, J.; Nelson, K. A. *Appl. Phys. Lett.* **2007**, *90*, 171121.
(6) Ignatiev, A.; Xu, Y. Q.; Wu, N. J.; Liu, D. *Mater. Sci. Eng.* **1998**, *B56*, 191–194.
(7) Pradarutti, B.; Matthaus, G.; Riehemann, S.; Notni, G.; Limpert, J.; Nolte, S.; Tunnermann, A. *J. Appl. Phys.* **2007**, *102*, 093105.
(8) Hebling, J.; Almasi, G.; Kozima, I. Z. *Opt. Express* **2002**, *10*, 1161–1166.
(9) Wang, T. D.; Lin, S. T.; Lin, Y. Y.; Chiang, A. C.; Huang, Y. C. *Opt. Express* **2008**, *16*, 6471–6478.
(10) Dawber, M.; Rabe, K. M.; Scott, J. F. *Rev. Mod. Phys.* **2005**, *77*, 1083–1130.
(11) Macutkevic, J.; Kamba, S.; Banys, J.; Brilingas, A.; Pashkin, A.; Petzelt, J.; Bormanis, K.; Sternberg, A. *Phys. Rev. B* **2006**, *74*, 104106.
(12) Macutkevic, J.; Kamba, S.; Banys, J.; Pashkin, A.; Bormanis, K.; Sternberg, A. *J. Eur. Ceram. Soc.* **2007**, *27*, 3713–3717.
(13) Macutkevic, J; Grigalaitis, R; Adomavicius, R; Krotkus, A.; Banys, J.; Valusis, G.; Bormanis, K.; Sternberg, A. *Phys. Status Solidi B* **2008**, *245*, 1206–1209.
(14) Parkinson, P.; Lloyd-Hughes, J.; Gao, Q.; Tan, H. H; Jagadish, C.; Johnston, M. B.; Herz, L. M. *Nano Lett.* **2007**, *7*, 2162–2165.
(15) Baxter, J.; Schmuttenmaer, C. A. *J. Phys. Chem. B* **2006**, *110*, 25229–25239.
(16) Bharadwaja, S. S. N.; Olszta, M.; Trolier-McKinstry, S.; Li, X.; Mayer, T. S.; Roozeboom, F. *J. Am. Ceram. Soc.* **2006**, *89*, 2695–2701.
(17) Lou, Y.; Szafraniak, I.; Zakharov, N. D.; Nagarajan, V.; Steinhart, M.; Wehrspohn, R. B.; Wendorff, J. H.; Ramesh, R.; Alexe, M. *Appl. Phys. Lett.* **2003**, *83*, 440–442.
(18) Nahata, A.; Weling, A. S.; Heinz, T. F. *Appl. Phys. Lett.* **1996**, *69*, 2321–2323.
(19) Peter, F.; Winnerl, S.; Schneider, H.; Helm, M.; Koehler, K. *Appl. Phys. Lett.* **2008**, *93*, 101102.
(20) Zhang, X. C.; Auston, D. H *J. Appl. Phys.* **1992**, *71*, 326–338.
(21) Chuang, S. L.; Schmitt-Rink, S.; Greene, B. I.; Saeta, P. N.; Levi, A. F. J. *Phys. Rev. Lett.* **1992**, *68*, 102–105.
(22) Dekorsy, T.; Auer, H.; Bakker, H. J.; Rostos, H. G.; Kurz, H. *Phys. Rev. B* **1996**, *53*, 4005–4014.
(23) Gu, P.; Tani, M.; Sakai, K.; Zhang, X. C. *J. Appl. Phys.* **2002**, *91*, 5533–5537.
(24) Scott, J. F. *Ferroelectric Memories*; Springer: Heidelberg, 2000; p 92.
(25) Goldman, S. R.; Kalikstein, K.; Kramer, B. *J. Appl. Phys.* **1978**, *49*, 2849–2854.
(26) Heyman, J. N.; Bell, D.; Khumalo, T. *Appl. Phys. Lett.* **2006**, *88*, 162104.
(27) Juan, P. C.; Chou, H. C.; Lee, J. Y. M. *Microelectron. Reliab.* **2005**, *45*, 1003–1006.
(28) Watanabe, Y.; Masuda, A. *Ferroelectrics* **2002**, *267*, 379–384.
(29) Watanabe, Y.; Urakami, Y.; Kaku, S. *Ferroelectrics* **2007**, *355*, 13–18.
(30) Watanabe, Y. *Top. Appl. Phys.* **2005**, *98*, 177–197.
(31) http://www.edinst.com.
(32) Mendis, R.; Smith, M. L.; Bignell, L. J.; Vickers, R. E. M.; Lewis, R. A. *J. Appl. Phys.* **2005**, *98*, 126104.
(33) Alexe, M.; Hesse, D.; Schmidt, V.; Senz, S.; Fan, H. J.; Zacharias, M.; Gösele, U. *Appl. Phys. Lett.* **2006**, *89*, 172907.
(34) Kim, J.; Yang, S. A.; Choi, Y. C.; Han, J. K.; Jeong, K. O.; Yun, Y. J.; Kim, J.; Yang, S. M.; Yoon, D.; Cheong, H.; Chang, K. S.; Noh, T. W.; Bu, S. D. *Nano Lett.* **2008**, *8*, 1813–1817.
(35) Tinkham, M.; Strandberg, M.W. P. *Phys. Rev.* **1955**, *97*, 951–966.
(36) Simon, S.; van der Pol, A.; Reijerse, E. J.; Kentgens, A. P. M.; van Moorsel, G. J.; de Boer, E. *J. Chem. Soc., Farady Trans.* **1994**, *90*, 2663–2670.
(37) Radford, H. E. *Phys. Rev.* **1961**, *122*, 114–130.
(38) Laguta, V. V.; Slipenyuk, A. M.; Bykov, I. P.; Glinchuk, M. D.; Maglione, M.; Michau, D.; Rosa, J.; Jastrabik, L. *Appl. Phys. Lett.* **2005**, *87*, 022903.
(39) Laguta, V. V.; Glinchuk, M. D.; Bykov, I. P.; Rosa, J.; Jastrabik, L.; Maksimenk, Yu. L. *Phys. Rev. B* **1966**, *54*, 12353–12360.
(40) Zhou, X. C.; Chen, X. S.; Lu, W. *Physica B* **2005**, *369*, 117–122.
(41) Mendis, R.; Smith, M. L.; Vickers, R. E. M.; Lewis, R. A.; Zhang, C. *Int. Conf. Terahertz Electron.* **2006**, 434.
(42) Krotkus, A.; Adomavicius, R.; Molis, G.; Urbanowicz, A.; Eusebe, H. *J. Appl. Phys.* **2004**, *96*, 4006–4008.
(43) Takahashi, K.; Kida, N.; Tonouchi, M. *Phys. Rev. Lett.* **2006**, *96*, 11740.
(44) Rana, D. S.; Kawayama, I.; Murakami, H.; Tonouchi, M. *Bull. Am. Phys. Soc.* **2008**, *53*, paper W37.012.
(45) Kamba, S.; Bovtun, V.; Petzelt, J.; Rychetsky, I.; Mizaras, R.; Brilingas, A.; Banys, J.; Grigas, J.; Kosec, M. *J. Phys.: Condens. Matter* **2000**, *12*, 497–519.

NL802277K